JPET Fast Forward. Published on January 28, 2021 as DOI: 10.1124/jpet.120.000217
This article has not been copyedited and formatted. The final version may differ from this version.

1. Title Page

Characterization of the onset, progression, and reversibility of morphological changes in mouse lung following pharmacological inhibition of LRRK2 kinase activity

Dianne K. Bryce[1], Chris M. Ware[1], Janice D. Woodhouse[2], Paul J. Ciaccio[3], J. Michael Ellis[4], Laxminarayan G. Hegde[2], Sabu Kuruvilla[5], Matthew L. Maddess[6], Carrie G. Markgraf[5], Karin M. Otte[7], Frederique M. Poulet[5], Lauren M. Timmins[1], Matthew E. Kennedy[1], Matthew J. Fell[1].

Merck & Co., Inc., Kenilworth, NJ USA

[1]Discovery Neuroscience, Merck & Co., Inc., Boston, MA, USA

[2]Pharmacology, Merck & Co., Inc., Boston, MA, USA

[3]Safety Assessment and Laboratory Animal Resources, Merck & Co., Inc., Boston, MA, USA

[4]Current affiliation: Bristol-Myers Squibb, Cambridge, MA, USA

[5]Safety Assessment and Laboratory Animal Resources, Merck & Co., Inc., West Point, PA, USA

[6]Discovery Chemistry, Merck & Co., Inc., Boston, MA, USA

[7]PPDM, Merck & Co., Inc., Boston, MA, USA

JPET Fast Forward. Published on January 28, 2021 as DOI: 10.1124/jpet.120.000217
This article has not been copyedited and formatted. The final version may differ from this version.

2. Running Title Page

a) LRRK2 Kinase Inhibition Affects Mouse Lung

b) Corresponding author:

a. Dianne Bryce, Merck & Co., Inc., 33 Avenue Louis Pasteur, Boston, MA 02115. USA
b. (860) 460-2412 (M)
c. Brycedk1@gmail.com

c)

Number of text pages: 19

Number of tables: 1

Number of figures: 5

Number of references: 25

Number of words in Abstract: 235

Number of words in Introduction: 722

Number of words in Discussion: 1542

Conflict of interest statement: All authors were or are employees of Merck Sharp & Dohme Corp., a subsidiary of Merck & Co., Inc., Kenilworth, NJ, USA and shareholders in Merck & Co., Inc., Kenilworth, NJ, USA at the time of their contributions

d) non-standard abbreviations:

e) recommended section: Drug Discovery and Translational Medicine

JPET Fast Forward. Published on January 28, 2021 as DOI: 10.1124/jpet.120.000217
This article has not been copyedited and formatted. The final version may differ from this version.

3. Abstract

Gain-of-function mutations in leucine-rich kinase 2 (LRRK2) are associated with increased incidence of Parkinson's disease (PD); thus, pharmacological inhibition of LRRK2 kinase activity is postulated as a disease modifying treatment for PD. Histomorphological changes in lungs of non-human primates (NHP) treated with small molecule LRRK2 kinase inhibitors have brought the safety of this treatment approach into question. While it remains unclear how LRRK2 kinase inhibition affects the lung, continued studies in NHPs prove to be both cost and resource prohibitive. To develop a tractable alternative animal model platform, we dosed male mice in-diet with the potent, highly selective LRRK2 kinase inhibitor MLi-2 and induced histomorphological changes in lung within one week. Oral bolus dosing of MLi-2, at a frequency modeled to provide steady-state exposure equivalent to that achieved with in-diet dosing, induced type II pneumocyte vacuolation, suggesting pulmonary changes require sustained LRRK2 kinase inhibition. Treating mice with MLi-2 in-diet for up to 6 months resulted in type II pneumocyte vacuolation which progressed only modestly over time and was fully reversible following withdrawal of MLi-2. Immunohistochemical analysis of lung revealed a significant increase in pro-surfactant protein C staining within type II pneumocytes. In the present study, we demonstrated the kinetics for onset, progression, and rapid reversibility of chronic LRRK2 kinase inhibitor effects on lung histomorphology in rodents and provide further evidence for the de-risking of safety and tolerability concerns for chronic LRRK2 kinase inhibition in PD.

JPET Fast Forward. Published on January 28, 2021 as DOI: 10.1124/jpet.120.000217
This article has not been copyedited and formatted. The final version may differ from this version.

4. Significance Statement

We have defined a mouse model by which the on-target lung effects of LRRK2 kinase inhibition can be monitored, whereas previous *in vivo* testing relied solely on non-human primates. Data serves to de-risk long-term treatment with LRRK2 kinase inhibitors, as all lung changes were mild and readily reversible.

JPET Fast Forward. Published on January 28, 2021 as DOI: 10.1124/jpet.120.000217
This article has not been copyedited and formatted. The final version may differ from this version.

5. Visual Abstract : NA

JPET Fast Forward. Published on January 28, 2021 as DOI: 10.1124/jpet.120.000217
This article has not been copyedited and formatted. The final version may differ from this version.

6. Introduction

Parkinson's disease is a debilitating, progressive movement disorder characterized by the loss of dopaminergic neurons in the substantia nigra pars compacta and is associated with the accumulation of alpha-synuclein containing protein aggregates termed Lewy bodies (Braak and Braak, 2000). Current therapies for PD target the dopaminergic system and have proven beneficial in the treatment of associated motor symptoms but do not impact disease progression (Ellis and Fell, 2017). With the incidence of PD expected to double by the year 2030, estimates indicate that the disease could afflict approximately 10 million patients worldwide (Dorsey et al., 2007), emphasizing the clear need to identify novel targets that can slow or stop disease progression.

One candidate that has emerged as a promising target for disease modification in PD is LRRK2. The *LRRK2* gene encodes a large multifunctional protein comprised of GTPase and kinase domains, flanked by several protein-protein interacting regions (Taylor and Alessi, 2020). Missense mutations in *LRRK2* are the leading cause of monogenic PD, accounting for ~4% of familial cases (Healy et al., 2008), and common variants in the *LRRK2* locus are known risk factors for PD. All pathogenic mutations in *LRRK2* (N1437H, R1441G/C/H, Y1699C, G2019S, and I2020T) increase kinase activity (West et al., 2005), and increased levels of LRRK2 kinase activity have been observed in post-mortem brain tissue from patients with idiopathic PD (Wang et al., 2017; Di Maio et al., 2018). Thus, inhibition of LRRK2 kinase activity represents a novel therapeutic strategy for slowing or stopping the progression of PD, not only in LRRK2 mutation carriers, but also potentially in the more common idiopathic forms of PD.

The ability to safely target LRRK2 kinase activity in the clinic has been called into question following studies, conducted in LRRK2-deficient rodents, which identified age-dependent phenotypes in both the kidney and lung. In LRRK2 knockout animals, hyaline droplets and lipofuscin-like brown pigment have been observed in in proximal renal tubular epithelium of the kidney, while enlarged and vacuolated type II pneumocytes with accumulation

JPET Fast Forward. Published on January 28, 2021 as DOI: 10.1124/jpet.120.000217
This article has not been copyedited and formatted. The final version may differ from this version.

of lamellar bodies are seen in the lung (Tong et al., 2010; Herzig et al., 2011; Baptista et al., 2013). Similar results have now been observed following dosing with small molecule LRRK2 kinase inhibitor compounds. Andersen and colleagues demonstrated the induction of a kidney phenotype in rats treated with the LRRK2 kinase inhibitor PFE-360 (Andersen et al., 2018). Importantly, these kidney changes were reversible and non-adverse. Efforts to assess the potential of LRRK2 kinase inhibitors to induce a lung phenotype similar to those observed in LRRK2 KO rodents have relied on studies in non-human primates (NHPs), since changes in the lungs of rodents following treatment with LRRK2 kinase inhibitor compounds (Daher et al., 2015; Fuji et al., 2015; Henderson et al., 2015) have not consistently been reported. In NHPs, two LRRK2 kinase inhibitors (GNE-7915 and GNE-0877) have been shown to induce type II pneumocyte vacuolation (Fuji et al., 2015). In a 2-week follow-up study in NHPs, the structurally distinct kinase inhibitors PFE-360 and MLi-2 also induced morphological changes in the lung, suggesting that the lung phenotype is an on-target effect of LRRK2 kinase inhibition (Scott et al., 2017). LRRK2 kinase inhibition in NHPs did not affect pulmonary function after 15 days of dosing, and the histomorphological changes were reversible following 2 weeks of recovery period (Baptista et al., 2020).

Given that PD is a progressive disorder that will require long-term treatment, understanding the potential for the lung morphological changes to progress with chronic inhibitor treatment has become critical. Efforts to evaluate this in preclinical studies are challenged by the reliance on NHPs as the responding species, and to date, 28 days is the longest treatment duration studied (Fuji et al., 2015; Baptista et al., 2020). In 2015, we observed the induction of lung morphological changes in mice following chronic (15 weeks) treatment with MLi-2, using an in-diet dosing paradigm (Fell et al., 2015). Here, we utilize an alternative animal model paradigm to perform a detailed characterization of the onset, progression, and reversibility of lung morphological changes by dosing MLi-2 in-diet for up to 6 months. These mouse studies yield reproducible, quantifiable endpoints which are similar to the effects on type II pneumocytes in

JPET Fast Forward. Published on January 28, 2021 as DOI: 10.1124/jpet.120.000217
This article has not been copyedited and formatted. The final version may differ from this version.

NHPs and provide a novel model to further investigate the relationship of LRRK2 kinase inhibition with lung changes that can be applied across novel compounds for treatment of PD.

JPET Fast Forward. Published on January 28, 2021 as DOI: 10.1124/jpet.120.000217
This article has not been copyedited and formatted. The final version may differ from this version.

7. Materials and Methods

Animals

All studies were carried out in accordance with the policies of the Animal Care and Use Committee of Merck Research Laboratories, Boston, MA, in conjunction with the American Association for the Accreditation of Laboratory Animal Care approved guidelines and the Guide for the Care and Use of Laboratory Animals. C57BL/6J male mice were received from Taconic Farms (Germantown, NY) at 6-8 weeks of age and were singly housed in an environmentally controlled room (temperature 22 ± 2°C and humidity >45%) on a 12-hour light-dark cycle. All mice were acclimated to the facility for a minimum of 5 days prior to the initiation of study, with standard diet (Teklad 2018sx from Envigo, Madison, WI) and water available *ad libitum*. Each treatment group consisted of 4 mice, except for the per os (PO) dosing and brochoalveolar lavage (BAL) collection studies which used 6 mice per treatment group.

Test Compound Formulation and Dosing Regimen

MLi-2 and GNE-7915 (Supplemental Figure 1) were synthesized at Merck Research Laboratories (Boston, MA). For PO dosing, MLi-2 was suspended in a beta-cyclodextrin derivative, Captisol (30% solution in water, Ligand Technologies, La Jolla, CA) and dosed at a volume of 10ml/kg. All other compound treatments were dosed in rodent chow, prepared at Research Diets (New Brunswick, NJ) and formulated to provided doses of 3, 10, 30, 60, or 120 mg/kg/day (MLi-2) or 10, 30, 100, 300 mg/kg/day (GNE-7915) based on an average daily food consumption of 3 grams. Mice were first habituated to vehicle diet (Research Diets D01060501) for 3 days. Chow was then substituted with formulated diet which was continued for 3-180 days, according to the study design. For some mice, a wash-out arm was conducted, returning mice to vehicle diet for 1 week. All mice and formulated chow were weighed weekly throughout the study to monitor appropriate weight gain and food consumption.

JPET Fast Forward. Published on January 28, 2021 as DOI: 10.1124/jpet.120.000217
This article has not been copyedited and formatted. The final version may differ from this version.

Terminal Tissue Collection

In order to preserve lung integrity for histological assessment, mice were anesthetized using isoflurane to effect, cervical dislocation was applied, and the caudal vena cava was severed to prevent the flow of blood into the base of the lung. One lobe of the lung was first tied off using surgical suture (Covidien Sofsilk^{TM}, New Haven, CT), then the trachea was cannulated, and the lungs inflated by injection of 1-2 ml 10% formalin. Lungs were then excised; the inflated lungs stored at room temperature (RT) in tubes containing additional 10% formalin and sent to Qualtek (Santa Barbara, CA) for embedding in paraffin and sectioning at 5 μm. The remaining (unfixed) lungs were quick-frozen on a steel plate resting on dry ice and stored at -80°C for analysis of pSer935 and total LRRK2 levels. For BAL collection, mice were euthanized with an intra-peritoneal (IP) injection of 0.1 ml Euthasol (Henry Schein, Melville NY). A small incision was made in the trachea, and 1 ml of saline was slowly lavaged through the lung, then re-collected into the syringe and placed in collection tubes. BAL fluid was centrifuged at 400 x *g* for 10 min at 4°C, and supernatants were collected and stored at -80°C.

Histopathological analysis and Image quantification

Formalin-fixed paraffin-embedded (FFPE) lung sections were either stained with hematoxylin and eosin (H&E) or immunohistochemically stained for pro-surfactant protein C (proSP-C) expression in type II pneumocytes. Immunohistochemical staining was carried out on a Ventana Discovery Ultra using the Chromomap detection method. Briefly, lung sections on glass slides were rehydrated, and heat induced epitope retrieval was performed using a Tris-borate EDTA solution. Slides were then incubated with an anti-proSP-C antibody (EMD Millipore; cat no. AB3786, 1:8000) followed by Discovery Omnimap anti-rabbit-HRP (Roche Tissue Diagnostics; cat no. 760-4311). Signal was visualized using the Discovery Chromomap DAB Kit (Ventana) and slides were counterstained with hematoxylin II (Ventana). The slides were digitized on a Leica XT scanning microscope (20x magnification), and the area of individual type II

JPET Fast Forward. Published on January 28, 2021 as DOI: 10.1124/jpet.120.000217
This article has not been copyedited and formatted. The final version may differ from this version.

pneumocytes in at least 10 randomly selected areas for each lung section was measured using HALO image analysis software version 2.1.1637 (Indica Labs, Corrales, NM).

Assessment of Plasma Levels of MLi-2 and GNE-7915

To define pharmacokinetic (PK) properties, mice were dosed PO with 30, 100, or 300 mg/kg MLi-2 and samples collected at 0.5, 1, 4, 8, and 24 hours post-dosing. Plasma samples were assayed for compound levels using liquid chromatography and tandem mass spectrometry analyses as previously described (Fell et al., 2015). For the modeling study, mice (n = 2) were orally dosed with 30, 100, and 300 mg/kg of MLi-2. Plasma was sampled at 1 and 8 hours, at 24 hours (1-day C_{max}), 120 and 128 hours (5 days, C_{max} and C_{min}), and 144 hours (C_{min}); terminal tissue and plasma samples were collected 12 hours following the last PO dosing in order to capture target engagement and histopathological changes at MLi-2 plasma exposure levels reflective of C_{min}. Corresponding blood levels were fitted to a one compartment model using Phoenix 64 (Build 6.3.0.395, WinNonlin version 6.3; Certara, Princeton, NJ). Blood levels of GNE-7915 mice dosed in-diet mice were detected as described (Fuji et al., 2015).

Western Blot

LRRK2 immunoblotting was run on samples from lung as described previously (Fell et al., 2015). Briefly, 100 µg of protein lysate was separated using 3-8% Tris-Acetate gels, then electrotransferred onto polyvinylidene difluoride membranes for 2 hours at 30V. Following blocking with 5% dry milk, blots were probed overnight at 4˚ C with either anti- phospho S935-LRRK2 antibody (1:1000 v/v, ab133450, Abcam, Cambridge, MA), anti-LRRK2 [MJFF2] antibody (1:500 v/v, ab133474, Abcam), or mouse anti-glyceraldehyde-3-phosphate dehydrogenase (GAPDH, 1:20,000 v/v, G8795, Sigma, St. Louis, MO). Membranes were washed with Tris-buffered saline plus Tween-20 (TBS-T) three times for 10 minutes, then incubated for one hour at RT with secondary antibody (donkey anti-rabbit IgG horseradish

JPET Fast Forward. Published on January 28, 2021 as DOI: 10.1124/jpet.120.000217
This article has not been copyedited and formatted. The final version may differ from this version.

peroxidase (1:2,000, Thermofisher); goat anti-mouse IgG IRDye 800CW (1:15,000, Li-Cor), or goat anti-mouse IgG IRDye 680RD (1:10,000, Li-Cor). Following three additional washes with TBS-T, blots were developed using SuperSignal enhanced chemiluminescence HRP substrate (ThermoFisher) and imaged on an Odyssey FC system. Image Studio (version 2.0) was used to quantify individual band intensity. The ratio of pSer935 LRRK2 to total LRRK2 protein levels was derived for each sample and expressed as a percentage of within-gel vehicle control lanes. When analyzing samples to assess changes in total LRRK2 protein levels, GAPDH was used as an internal reference protein.

Quantification of Surfactant Protein D Levels in BAL fluid

For collected BAL fluid, samples were assayed using an ELISA kit specific for mouse Surfactant Protein-D (SP-D, R&D Systems Inc.; Quantikine MFSPD0, Minneapolis, MN) according to insert directions using a 1:500 dilution of BAL fluid.

Statistical Analysis

Data were analyzed using one-way analysis of variance (ANOVA) with Dunnett's post-hoc test, comparing treatment groups to vehicle controls (GraphPad Prism Software, Inc., version 7.02). For studies comparing multiple dosing time points, a two-way ANOVA was used with Dunnett's multiple comparison test for post-hoc analysis; level of significance was set to 0.05. Data were represented as mean values ± the standard error of the mean (SEM), and the level of significant differences between means was depicted using ***$P < 0.001$, **$P < 0.01$, and *$P < 0.05$.

JPET Fast Forward. Published on January 28, 2021 as DOI: 10.1124/jpet.120.000217
This article has not been copyedited and formatted. The final version may differ from this version.

8. Results

Effects of MLi-2 on Phosphorylation of Ser935 LRRK2 in Mouse Lung and Early Detection of Lung Histomorphological Changes Following 7 Days of In-diet Dosing

To define the pharmacokinetic and pharmacodynamic (PK/PD) relationship of MLi-2 in C57BL/6J mice and to probe for early indications of pulmonary changes, we first treated mice in-diet for 7 days with a range of doses of MLi-2 (3, 10, 30, 60, or 120 mg/kg/day). Consistent with previous findings, MLi-2 was well-tolerated and resulted in normal body weight (BW) gains for all groups (Supplemental Figure 1A). MLi-2 administration resulted in a dose-dependent reduction in the phosphorylation of LRRK2 Ser935 in lung at doses of 30, 60, and 120 mg/kg/day [$F(5,18)=39.3$; $P < 0.0001$, and no significant decreases in total LRRK2 protein levels were detected (Supplemental Figure 1C).

Histopathological assessment of H&E stained sections revealed minimal enlargement of randomly scattered alveolar epithelial cells having features consistent with type II pneumocytes in the lungs of mice treated with doses of 60 and 120 mg/kg/day for 7 days (Figure 2A). As compared to vehicle treated mice, an increase in both size and number of clear round vacuoles induced distension of the cytoplasm that resulted in an increased prominence of many of the type II pneumocytes. As type II pneumocytes are the primary source of lung surfactant that is released from vesicles and this is required to maintain tissue compliance, we assessed tissue sections for the surfactant associated protein proSP-C. Immunohistochemical analysis revealed proSP-C immunoreactivity was localized exclusively to type II pneumocytes and appeared elevated in proportion to the increase in intracellular vesicles observed by H&E (Figure 2B). No changes in lung (H&E or proSP-C staining) were observed at the 3, 10, and 30 mg/kg/day doses, while significant increases were seen in both 60 and 120 mg/kg/day doses (Table 1). Relating free unbound plasma concentrations of MLi-2 to peripheral target engagement, we derived the pSer935 LRRK2 IC_{50} in lung to be 1.3 nM and thus morphological changes are

JPET Fast Forward. Published on January 28, 2021 as DOI: 10.1124/jpet.120.000217
This article has not been copyedited and formatted. The final version may differ from this version.

observed in lung only when plasma levels are sustained and exceed the lung pSer935 LRRK2 IC_{50} ≥3-fold.

Modeling Exposure Using PO Dosing: Effects of MLi-2 on Lung Target Engagement and Morphological Changes Following 7 Days of PO Dosing (150 mg/kg BID)

Several studies have described a lack of LRRK2-induced morphological changes in rodent lung following oral dosing with LRRK2 kinase inhibitor compounds (Fuji et al., 2015; Henderson et al., 2015; Andersen et al., 2018). MLi-2 dosed QD for 30 days at 30 mg/kg PO (the IC_{90} for pSer935 LRRK2 inhibition at 1 hour in lung) was without effect in C57BL/6J lung (internal unpublished data); however, 30 mg/kg/day of MLi-2 delivered in-diet was shown to induce morphological changes in lung of Mitopark mice (Fell et al., 2015). Given rodent lung alterations have only ever been noted following in-diet dosing, we hypothesized that maintenance of a minimal threshold of LRRK2 kinase inhibition is necessary in order to provoke the enlargement of type II pneumocytes. A comparison of time versus exposure profiles of 30 and 60 mg/kg/day MLi-2 dosed in-diet with a bolus oral dose of 30 mg/kg over a 24-hour period (Fig 2A) demonstrated that in-diet dosing provided sustained drug exposure in plasma, with minimal peak-to-trough variation relative to bolus delivery. Pharmacokinetic modeling was performed to determine an appropriate dose in mouse to attain steady-state C_{min} levels comparable to those observed with 60 mg/kg/day of in-diet dosing, the minimal dose of MLi-2 that induced the enlargement of type II pneumocytes. The predicted oral dose to yield blood C_{min} at a steady-state level of 2.6 µM (or 19.8 nM free plasma concentration) was 150 mg/kg BID (Figure 2B). Accordingly, one group of mice was dosed orally BID with 150 mg/kg MLi-2 for 7 days; vehicle and parallel 60 mg/kg/day MLi-2 in-diet control groups were also dosed. No tolerability issues were noted in any of the treatment groups. Frequent plasma sampling from the PO-dosed mice confirmed that the model adequately predicted exposures and the minimal

JPET Fast Forward. Published on January 28, 2021 as DOI: 10.1124/jpet.120.000217
This article has not been copyedited and formatted. The final version may differ from this version.

exposure levels observed were always maintained above the lower threshold of 19.8 nM free plasma MLi-2 (Figure 2B).

As depicted in Figure 2C, both PO (150 mg/kg BID) and in-diet (60 mg/kg/day) treatments resulted in the significant inhibition of pSer935 LRRK2 in lung [$F(2,11)=602.2$; $P < 0.0001$]. No significant changes were detected in total LRRK2 protein levels; values were comparable to those obtained for control mice in lung [$F(2,11)=0.83$; ns].

Histopathological analysis of the H&E stained sections revealed that 150 mg/kg MLi-2 PO BID was associated with enlargement of type II pneumocytes in all mice after 7 days of treatment; also noted was an increase in the number and size of vacuoles, as compared to vehicle treated mice (Figure 1A). One-way ANOVA analysis of IHC staining for proSP-C (Figure 1B) showed a significant increase in both PO and in-diet dosed groups (Figure 2D); Dunnett's Post-Hoc analysis resulted in $P < 0.05$ for in-diet treatment and $P < 0.01$ for PO dosed mice.

Effects of a Structurally Distinct LRRK2 Kinase Inhibitor (GNE-7915) on Biochemical and Immunohistochemical Endpoints in Mouse Lung Following 7 Days of In-Diet Dosing

We next assessed whether morphological changes in lungs of mice could be induced using a structurally distinct LRRK2 kinase inhibitor. GNE-7915 is a small molecule LRRK2 kinase inhibitor that demonstrates potency, selectivity, and brain penetrability (Fuji et al., 2015). Whereas GNE-7915 was shown to induce lung effects following 7 days of treatment in NHPs at doses ≥ 25 mg/kg/day, studies conducted in mice (up to 300 mg/kg PO BID for 15 days) and rats (up to 100 mg/kg QD for 7 days) did not result in microscopic changes in lung. Here we proposed that using formulated chow to dose GNE-7915 in-diet would achieve sustained plasma levels without incurring tolerability issues. Mice received 10, 30, 100, or 300 mg/kg/day of GNE-7915 in-diet for 7 days. Following a brief drop in food intake during days 1-3 of transition to formulated diet, all mice returned to normal BW by day 7 (Supplemental Figure 1B). In order to measure both early and terminal compound exposure, plasma levels were assayed following

JPET Fast Forward. Published on January 28, 2021 as DOI: 10.1124/jpet.120.000217
This article has not been copyedited and formatted. The final version may differ from this version.

3- or 7- days of in-diet dosing. Free plasma exposures of GNE-7915 were stable across days and ranged from 10 nM-28 nM (Table 1). Analysis of western blot images (Figure 3A) showed GNE-7915 significantly inhibited pSer935 LRRK2 in a dose-dependent manner in lung [$F(4,14=28.3$; $P < 0.0001$], with no significant reduction in total protein levels [$F(4,14)=0.83$, ns] (Figure 3B). Plotting the PK versus PD response (unbound free plasma levels vs tissue pSer935-LRRK2) yielded the GNE-7915 IC_{50} to be 12.8 nM in lung. Thus, peripheral exposure to GNE-7915 reached 2.5-fold over the lung IC_{50} at the maximum tested dose of GNE-7915 (Figure 3C). Analysis of H&E stained sections reported 1 of 4 treated mice at the highest dose of GNE-7915 (300 mg/kg/day) demonstrated increased vacuolation of type II pneumocytes (Table 1, Figure 1A). The positive control MLi-2 (120 mg/kg/day) showed increased vacuolation typical of this dose, while vehicle and other doses of GNE-7915 were without notable lung histology findings. Post-hoc analysis of proSP-C IHC staining (Figure 1B) indicated significant increases above vehicle only at 300 mg/kg/day GNE-7915 [$F(4,15)=6.9$; $P < 001$]; Dunnett's test at 300 mg/kg/day $P < 0.01$ (Figure 3D).

Defining the Time Course and Progression of Lung Effects in Mice Treated with MLi-2 From 3 to 180 Days

To define the earliest detectable changes in lung following initiation of LRRK2 kinase inhibition, to monitor the progression of lung changes following chronic dosing, and to investigate reversibility upon compound withdrawal, mice were dosed in–diet with either 30, 60, or 120 mg/kg/day of MLi-2 for intervals ranging from 3 days to 6 months. One arm of the study included a wash-out phase, where medicated diet was replaced with vehicle diet for 7 days prior to collection of tissues. MLi-2 was well tolerated, with no adverse events being noted in any group for the duration of the study. Inhibition of pSer935 LRRK2 in lung remained relatively constant throughout the treatment phase of the study; a two-way ANOVA revealed a significant effect of dose ([$F(2,52=662.1$; $P < 0.0001$]) and no effect of time on-diet (lung [$F(5,52=0.33$

JPET Fast Forward. Published on January 28, 2021 as DOI: 10.1124/jpet.120.000217
This article has not been copyedited and formatted. The final version may differ from this version.

P=0.89]). Total LRRK2 levels in lung tissue were unchanged following chronic treatment with drug with the exception of a transient, significant reduction noted in the 120 mg/kg/day group at the single time point of 7 days ((*F*(5,52)=2.78 P=0.027) in this study.

Microscopic examination of H&E stained sections of lungs from mice treated with 30 mg/kg/day MLi-2 revealed no morphological changes at any time point. LRRK2 kinase inhibitor-induced changes in lung were evident after 3 days of dosing at 60- and 120 mg/kg/day, and persisted at 7, 14, 28, 90, and 180 days on-diet. There were no degenerative or inflammatory changes at any of the times examined, and the changes neither progressed nor worsened with the extended compound treatment.

Quantification of the area of the type II pneumocytes (Figure 4) showed dose-related increases in surfactant protein C immunoreactivity (two-way ANOVA drug [$F(3,67) = 94.0$; $P < 0.0001$], time [$F(5,67) = 6.46$; $P < 0.0001$], and drug × time interaction [$F(15,67) = 2.45$; $P < 0.01$]). While the 30 mg/kg/day dose was without effect at all times studied, the 120 mg/kg/day dose induced significant increases in proSP-C within 3 days of treatment and remained significantly elevated for 6 months (Dunnett's post-test $P < 0.0001$), consistent with the observation of type II pneumocyte vacuolation upon H&E analysis. Lungs of mice treated with the intermediate dose of MLi-2 (60 mg/kg/day) showed significant increases in proSP-C staining at 7 days and a peak response at 28 days; this effect then regressed at 90 and 180 days such that by the 6-month timepoint, proSP-C staining was equivalent to that of vehicle treated mice (P=0.12 at 3 days; $P < 0.0001$ from 7-60 days; P=0.0001 at 90 days; P=0.084 at 180 days).

Histomorphological and Biochemical Changes are Reversible

In order to study the reversibility of the observed lung phenotype, lungs and plasma were collected and assayed following a 7 day washout of MLi-2 after 28, 90, and 180 days of dosing in-diet. After 28 dosed days with a one-week washout, lung pSer935/total LRRK2 reverted to vehicle levels (Supplemental Figure 2). Following 90 days or 180 days of LRRK2

JPET Fast Forward. Published on January 28, 2021 as DOI: 10.1124/jpet.120.000217
This article has not been copyedited and formatted. The final version may differ from this version.

kinase inhibitor treatment with a 7 day washout, the ratio of pSer935/total LRRK2 significantly exceeded control values at 60 mg/kg/day ($P < 0.01$ at both time points) and 120 mg/kg/day ($P < 0.05$ at 90 days). An examination of the western blot images suggested that this effect was driven by a disproportionate increase in pSer935 LRRK2, although verification of any apparent increase in kinase activity would need to be validated by studying the direct phosphorylation site, Ser1292 LRRK2. Analysis of terminal plasma samples from these mice were consistent with previously observed levels of MLi-2 at the 60- and 120 mg/kg/day doses, and after the washout period, levels of MLi-2 were below the detection limit of the assay (2.5 nM).

H&E stained lung sections revealed no differences between MLi-2-treated mice (30 mg/kg/day) and vehicle throughout the study at all time points. With both 60 and 120 mg/kg/day, 4/4 lungs displayed enlarged type II pneumocytes at all time points (28, 90, 180 days), except for the 28-day at 60 mg/kg/day treatment group in which 3/4 mice showed histomorphological changes. Complete recovery was observed following the 7 day washout period for all chronic dosing groups: 28 days, 3 months, and 6 months dosing at 60 and 120 mg/kg/day (Figure 5A depicts 120 mg/kg/day). Quantification of proSP-C (Figure 5B) depicted a significant increase in type II pneumocyte area following 28 and 90 days with 60 mg/kg/day, and at 28, 90, and 180 days at 120 mg/kg/day ($P < 0.01$ where significant). Consistent with the reversal of the enlarged type II pneumocyte morphology observed by histomorphological examination, proSP-C positive area in the lungs of MLi-2 treated groups in the 28, 90, and 180-day wash-out arms was not different from controls. To determine whether the observed increases in proSP-C could be indicative of decreased surfactant secretion, we measured SP-D levels in BAL fluid from mice that had been dosed in-diet for 28 days, and from mice in the washout arm of that study. No changes were detected in SP-D levels in BAL fluid from mice treated with 30, 60, and 120 mg/kg/day (one-way ANOVA, P=0.65) nor following washout of MLi-2 (P=0.28), thus intracellular accumulation of surfactant proteins caused by LRRK2 kinase inhibition does not appear to result from impaired secretion (Figure 5C).

JPET Fast Forward. Published on January 28, 2021 as DOI: 10.1124/jpet.120.000217
This article has not been copyedited and formatted. The final version may differ from this version.

JPET Fast Forward. Published on January 28, 2021 as DOI: 10.1124/jpet.120.000217
This article has not been copyedited and formatted. The final version may differ from this version.

8. Discussion

Inhibition of LRRK2 kinase activity has emerged as an attractive target for slowing the progression of PD in not only LRRK2 mutation carriers, but also patients with idiopathic PD (Di Maio et al., 2018). Short-term LRRK2 kinase inhibitor treatment in NHPs leads to increased type II pneumocyte vacuolation in the lung, raising concerns about the ability to safely inhibit LRRK2 kinase activity in the clinic (Fuji et al., 2015). Here we successfully induced morphological changes in mouse lung following LRRK2 kinase inhibitor treatment and provided further evidence to allay lung safety concerns. First, we demonstrated that 7-days treatment with the LRRK2 kinase inhibitor MLi-2, via in-diet or PO dosing, is sufficient to cause lung changes in mice, but only at doses which provide complete and sustained inhibition of LRRK2. Next, dosing MLi-2 for up to six months induced changes in lung morphology that occurred rapidly, progressed only slightly, and after 6 months treatment, stained for pro-surfactant protein C at levels indistinguishable from control mice. Third, no detectable changes in SP-D levels were identified in the BAL fluid of mice in which the morphological change was confirmed. Finally, the morphological changes induced by MLi-2 treatment were rapidly reversible upon one-week withdrawal such that, irrespective of MLi-2 treatment duration, normal type II pneumocyte morphology and proSP-C levels were restored. Therefore, lung responses to LRRK2 kinase inhibition reflect rapid, adaptive responses that do not progress and are quickly reversed upon cessation of drug treatment.

In contrast to NHP studies, where LRRK2 kinase inhibitor-induced lung changes were noted within 7 days of oral dosing (Fuji et al., 2015; Baptista et al., 2020), visualization of similar pharmacologically-induced alterations in rodent lung has proven challenging (Daher et al., 2015; Fuji et al., 2015; Andersen et al., 2018; Kelly et al., 2018). We hypothesized that the transient inhibition of kinase activity achieved with PO dosing in rodents is not sufficient to induce morphological changes in lung; rather a sustained, minimal trough level of LRRK2 kinase

JPET Fast Forward. Published on January 28, 2021 as DOI: 10.1124/jpet.120.000217
This article has not been copyedited and formatted. The final version may differ from this version.

inhibition is required. This “time on target” hypothesis could be readily tested in mice using in-diet dosing. Indeed, one-week of in-diet dosing with MLi-2 enabled us to define the relationship between plasma exposure, and level of LRRK2 kinase inhibition and morphological changes in the lung. Importantly, no changes in lung were observed with 30 mg/kg/day dosing, which produced a C_{trough} exposure of 2.8X of the LRRK2 pSer935 IC_{50}, yet changes were observed at 60 and 120 mg/kg/day, when C_{trough} exposures reached 6x and 20x of the LRRK2 pSer935 IC_{50} respectively. In-diet dosing for 7 days with the structurally distinct GNE-7915 induced a significant increase in proSP-C at 300 mg/kg/day, and, combined with the presence of enlarged type II pneumocytes in one of the four mice tested, demonstrated that the lung phenotype was an on-target effect of LRRK2 kinase inhibition. Next, we modeled a PO dosing regimen to maintain MLi-2 plasma exposure above the hypothesized C_{trough}. Not only did we achieve the targeted unbound plasma levels, mimicking that of the 60 mg/kg/day dose in-diet, but we successfully demonstrated LRRK2 kinase inhibitor-induced enlargement of type II pneumocytes following oral gavage dosing along with associated increases in proSP-C. Collectively, these data established that the lung phenotype induced by LRRK2 kinase inhibitors can be observed in mice provided that the plasma exposure is maintained above a minimal threshold. In the case of MLi-2 this threshold is at least >3X the LRRK2 pSer935 IC_{50}. One limitation of our studies is that only male mice were tested. While both sexes were equally represented in NHP lung histopathology and toxicology studies with no differences noted (Baptista et al., 2020), additional testing is necessary to extend our findings here across sex.

Having established this lung phenotype in mice, we next sought to leverage this model to perform a detailed kinetic analysis of the onset, progression, and reversibility of the lung morphological changes. At the lowest in-diet dose (30 mg/kg/day), near complete inhibition of LRRK2 kinase activity was achieved in the periphery, yet no lung histomorphological changes were detected even after 6 months on-diet. Importantly, at this dose high levels of brain target engagement were observed (~55-85% inhibition of pSer935). These results are consistent with

JPET Fast Forward. Published on January 28, 2021 as DOI: 10.1124/jpet.120.000217
This article has not been copyedited and formatted. The final version may differ from this version.

recent observations in NHPs (Baptista et al., 2020) which showed that lower doses of MLi-2 and the structurally distinct inhibitor PFE-360 achieved high levels of LRRK2 kinase inhibition in the brain (>50% inhibition of pSer935) and did not produce the lung phenotype. Although levels of LRRK2 kinase activity required to impact disease progression in PD patients is yet to be determined, these data collectively suggest that it may be feasible to achieve a margin between high levels of brain LRRK2 kinase inhibition and the induction of the lung phenotype.

Higher doses of MLi-2 (60 and 120 mg/kg/day) produced maximal LRRK2 kinase inhibition and elicited morphological changes in type II pneumocytes of lungs in as little as 3 days; this change did not progress in size or number of vacuoles in type II pneumocytes over 6 months of sustained LRRK2 kinase inhibition. Moreover, the increase in proSP-C that accompanied these changes was modest, progressed only slightly from day 3 to day 28, and regressed over time such that following 6 months on-diet, proSP-C levels in the 60 mg/kg/day group were indistinguishable from those of controls. Regression in the 60 mg/kg/day group likely suggests that type II pneumocyte trafficking of surfactant can adapt to chronic high levels of LRRK2 kinase inhibition. Importantly, the induction of the lung phenotype was rapidly reversed when inhibition was released such that all morphological changes completely recovered within one week of compound wash-out. Taken together, these data indicate a dynamic, adaptive response to kinase inhibition and suggest that full recovery can be rapidly achieved upon stopping treatment. Our findings in mice support those of Baptista et al., (2020) who determined the lung phenotype in NHPs to be completely reversible following a 14-day recovery period.

Pulmonary surfactant protein D levels have been assessed as a potential biomarker of lung function in pulmonary disorders such as COPD (Sorensen, 2018). Here, we saw no changes in SP-D levels in BAL fluid regardless of dose or duration of treatment, suggesting that LRRK2 kinase inhibition does not affect surfactant levels in the alveolar space. However, considering the role of LRRK2 in facilitating not only the synthesis and secretion, but also the reuptake and reprocessing of surfactant by type II pneumocytes, additional investigation is

JPET Fast Forward. Published on January 28, 2021 as DOI: 10.1124/jpet.120.000217
This article has not been copyedited and formatted. The final version may differ from this version.

necessary to fully understand the kinetics of surfactant metabolism with LRRK2 kinase inhibition. Although we have conducted a detailed histomorphological characterization of the lung phenotype, we have not assessed the impact of LRRK2 kinase inhibition on pulmonary function in mice. The functional effects of LRRK2 kinase inhibition have recently been evaluated in NHPs (Baptista et al., 2020) and in humans in an 11-day phase 1b study with DNL-201, with no dose dependent changes to pulmonary function observed. Finally, loss of function variants in LRRK2 are not strongly associated with any adverse phenotypes (Whiffin et al., 2020).

Inhibition of LRRK2 kinase activity results in the destabilization of the LRRK2 protein (Herzig et al., 2011; Zhao et al., 2015; Lobbestael et al., 2016) and it has been suggested that inhibitor-induced reductions in LRRK2 protein levels are critical to the induction of the lung phenotype. (Herzig et al., 2011)(Herzig et al., 2011)(Herzig et al., 2011)Here, we demonstrated the emergence of lung effects within 3 days of dosing, yet a decrease in lung total LRRK2 protein was only observed at a single (7 day) timepoint in one study. Our data not only suggest that inhibitor-induced decreases in protein levels are not likely to be exclusively responsible for the induction of lung histomorphological changes, but also confirm previous reports which observed the induction of the lung phenotype in NHPs without attendant alterations in total LRRK2 levels (Fuji et al., 2015; Baptista et al., 2020). While the underlying molecular mechanism by which inhibition of LRRK2 kinase activity leads to accumulation of surfactant proteins in type II pneumocyte remains unclear, alterations in the endolysosomal pathway may be involved. LRRK2 has been shown to phosphorylate a subset of Rab GTPases (Steger et al., 2016), which play a critical role in regulating vesicular trafficking. Specifically, phosphorylation at Thr-73 on Rab10 blocks its interaction with GDP dissociation inhibitors leading to the accumulation of membrane-bound, inactive Rab proteins (Eguchi et al., 2018). We propose that near complete inhibition of LRRK2 kinase activity may also disrupt the balance of membrane-bound active vs inactive Rab proteins, leading to lysosomal dysfunction and the emergence of

JPET Fast Forward. Published on January 28, 2021 as DOI: 10.1124/jpet.120.000217
This article has not been copyedited and formatted. The final version may differ from this version.

the lung phenotype. Studies to further explore the molecular mechanism of the lung morphological changes in response to LRRK2 kinase inhibitor treatment are currently underway. Sustained and complete inhibition of LRRK2 kinase activity leads to the rapid induction of a lung phenotype in mice. These lung changes do not progress over 6 months of treatment and are without measurable impact on surfactant protein D secretion. Importantly, this lung phenotype rapidly normalizes upon cessation of compound administration. While monitoring pulmonary function will be a key component in LRRK2 kinase inhibitor clinical studies, these data, combined with results from the MJFF LRRK2 Safety Initiative in NHP, suggest that the morphological changes in type II pneumocytes should not prevent the continued clinical evaluation of LRRK2 kinase inhibitors for PD.

10. Acknowledgements

The authors thank Cheryl Leyns for her assistance in formatting western blot images for this manuscript.

JPET Fast Forward. Published on January 28, 2021 as DOI: 10.1124/jpet.120.000217
This article has not been copyedited and formatted. The final version may differ from this version.

11. Author Contributions

Participated in research design: Bryce, Fell, Hegde, and Otte.

Conducted experiments: Bryce, Woodhouse, and Timmins.

Contributed new reagents or analytic tools*:* Ellis and Maddess.

Performed data analysis: Bryce, Ware, Ciaccio, Kuruvilla, Markgraf, Otte, Poulet, and Timmins*.*

Wrote or contributed to the writing of the manuscript: Bryce, Fell, Ware, Otte, and Kennedy.

JPET Fast Forward. Published on January 28, 2021 as DOI: 10.1124/jpet.120.000217
This article has not been copyedited and formatted. The final version may differ from this version.

12. References

Andersen MA, Wegener KM, Larsen S, Badolo L, Smith GP, Jeggo R, Jensen PH, Sotty F, Christensen KV and Thougaard A (2018) PFE-360-induced LRRK2 inhibition induces reversible, non-adverse renal changes in rats. *Toxicology* **395**:15-22.

Baptista MA, Dave KD, Frasier MA, Sherer TB, Greeley M, Beck MJ, Varsho JS, Parker GA, Moore C, Churchill MJ, Meshul CK and Fiske BK (2013) Loss of leucine-rich repeat kinase 2 (LRRK2) in rats leads to progressive abnormal phenotypes in peripheral organs. *PloS one* **8**:e80705.

Baptista MAS, Merchant K, Barrett T, Bhargava S, Bryce DK, Ellis JM, Estrada AA, Fell MJ, Fiske BK, Fuji RN, Galatsis P, Henry AG, Hill S, Hirst W, Houle C, Kennedy ME, Liu X, Maddess ML, Markgraf C, Mei H, Meier WA, Needle E, Ploch S, Royer C, Rudolph K, Sharma AK, Stepan A, Steyn S, Trost C, Yin Z, Yu H, Wang X and Sherer TB (2020) LRRK2 inhibitors induce reversible changes in nonhuman primate lungs without measurable pulmonary deficits. *Science translational medicine* **12**.

Braak H and Braak E (2000) Pathoanatomy of Parkinson's disease. *J Neurol* **247 Suppl 2**:II3-10.

Daher JP, Abdelmotilib HA, Hu X, Volpicelli-Daley LA, Moehle MS, Fraser KB, Needle E, Chen Y, Steyn SJ, Galatsis P, Hirst WD and West AB (2015) Leucine-rich Repeat Kinase 2 (LRRK2) Pharmacological Inhibition Abates alpha-Synuclein Gene-induced Neurodegeneration. *The Journal of biological chemistry* **290**:19433-19444.

Di Maio R, Hoffman EK, Rocha EM, Keeney MT, Sanders LH, De Miranda BR, Zharikov A, Van Laar A, Stepan AF, Lanz TA, Kofler JK, Burton EA, Alessi DR, Hastings TG and Greenamyre JT (2018) LRRK2 activation in idiopathic Parkinson's disease. *Science translational medicine* **10**.

Dorsey ER, Constantinescu R, Thompson JP, Biglan KM, Holloway RG, Kieburtz K, Marshall FJ, Ravina BM, Schifitto G, Siderowf A and Tanner CM (2007) Projected number of people with Parkinson disease in the most populous nations, 2005 through 2030. *Neurology* **68**:384-386.

Eguchi T, Kuwahara T, Sakurai M, Komori T, Fujimoto T, Ito G, Yoshimura SI, Harada A, Fukuda M, Koike M and Iwatsubo T (2018) LRRK2 and its substrate Rab GTPases are sequentially targeted onto stressed lysosomes and maintain their homeostasis. *Proc Natl Acad Sci U S A* **115**:E9115-E9124.

Ellis JM and Fell MJ (2017) Current approaches to the treatment of Parkinson's Disease. *Bioorg Med Chem Lett* **27**:4247-4255.

Fell MJ, Mirescu C, Basu K, Cheewatrakoolpong B, DeMong DE, Ellis JM, Hyde LA, Lin Y, Markgraf CG, Mei H, Miller M, Poulet FM, Scott JD, Smith MD, Yin Z, Zhou X, Parker EM, Kennedy ME and Morrow JA (2015) MLi-2, a Potent, Selective, and Centrally Active Compound for Exploring the Therapeutic Potential and Safety of LRRK2 Kinase Inhibition. *The Journal of pharmacology and experimental therapeutics* **355**:397-409.

Fuji RN, Flagella M, Baca M, Baptista MA, Brodbeck J, Chan BK, Fiske BK, Honigberg L, Jubb AM, Katavolos P, Lee DW, Lewin-Koh SC, Lin T, Liu X, Liu S, Lyssikatos JP, O'Mahony J, Reichelt M, Roose-Girma M, Sheng Z, Sherer T, Smith A, Solon M, Sweeney ZK, Tarrant J, Urkowitz A, Warming S, Yaylaoglu M, Zhang S, Zhu H, Estrada AA and Watts RJ (2015) Effect of selective LRRK2 kinase inhibition on nonhuman primate lung. *Science translational medicine* **7**:273ra215.

Healy DG, Falchi M, O'Sullivan SS, Bonifati V, Durr A, Bressman S, Brice A, Aasly J, Zabetian CP, Goldwurm S, Ferreira JJ, Tolosa E, Kay DM, Klein C, Williams DR, Marras C, Lang AE, Wszolek ZK, Berciano J, Schapira AH, Lynch T, Bhatia KP, Gasser T, Lees AJ, Wood NW and International LC (2008) Phenotype, genotype, and worldwide genetic penetrance of LRRK2-associated Parkinson's disease: a case-control study. *The Lancet* **7**:583-590.

Henderson JL, Kormos BL, Hayward MM, Coffman KJ, Jasti J, Kurumbail RG, Wager TT, Verhoest PR, Noell GS, Chen Y, Needle E, Berger Z, Steyn SJ, Houle C, Hirst WD and Galatsis P (2015) Discovery and preclinical profiling of 3-[4-(morpholin-4-yl)-7H-pyrrolo[2,3-d]pyrimidin-5-yl]benzonitrile (PF-

06447475), a highly potent, selective, brain penetrant, and in vivo active LRRK2 kinase inhibitor. *Journal of medicinal chemistry* **58**:419-432.

Herzig MC, Kolly C, Persohn E, Theil D, Schweizer T, Hafner T, Stemmelen C, Troxler TJ, Schmid P, Danner S, Schnell CR, Mueller M, Kinzel B, Grevot A, Bolognani F, Stirn M, Kuhn RR, Kaupmann K, van der Putten PH, Rovelli G and Shimshek DR (2011) LRRK2 protein levels are determined by kinase function and are crucial for kidney and lung homeostasis in mice. *Human molecular genetics* **20**:4209-4223.

Kelly K, Wang S, Boddu R, Liu Z, Moukha-Chafiq O, Augelli-Szafran C and West AB (2018) The G2019S mutation in LRRK2 imparts resiliency to kinase inhibition. *Exp Neurol* **309**:1-13.

Lobbestael E, Civiero L, De Wit T, Taymans JM, Greggio E and Baekelandt V (2016) Pharmacological LRRK2 kinase inhibition induces LRRK2 protein destabilization and proteasomal degradation. *Scientific reports* **6**:33897.

Scott JD, DeMong DE, Greshock TJ, Basu K, Dai X, Harris J, Hruza A, Li SW, Lin SI, Liu H, Macala MK, Hu Z, Mei H, Zhang H, Walsh P, Poirier M, Shi ZC, Xiao L, Agnihotri G, Baptista MA, Columbus J, Fell MJ, Hyde LA, Kuvelkar R, Lin Y, Mirescu C, Morrow JA, Yin Z, Zhang X, Zhou X, Chang RK, Embrey MW, Sanders JM, Tiscia HE, Drolet RE, Kern JT, Sur SM, Renger JJ, Bilodeau MT, Kennedy ME, Parker EM, Stamford AW, Nargund R, McCauley JA and Miller MW (2017) Discovery of a 3-(4-Pyrimidinyl) Indazole (MLi-2), an Orally Available and Selective Leucine-Rich Repeat Kinase 2 (LRRK2) Inhibitor that Reduces Brain Kinase Activity. *Journal of medicinal chemistry* **60**:2983-2992.

Sorensen GL (2018) Surfactant Protein D in Respiratory and Non-Respiratory Diseases. *Front Med (Lausanne)* **5**:18.

Steger M, Tonelli F, Ito G, Davies P, Trost M, Vetter M, Wachter S, Lorentzen E, Duddy G, Wilson S, Baptista MA, Fiske BK, Fell MJ, Morrow JA, Reith AD, Alessi DR and Mann M (2016) Phosphoproteomics reveals that Parkinson's disease kinase LRRK2 regulates a subset of Rab GTPases. *eLife* **5**.

Taylor M and Alessi DR (2020) Advances in elucidating the function of leucine-rich repeat protein kinase-2 in normal cells and Parkinson's disease. *Curr Opin Cell Biol* **63**:102-113.

Tong Y, Yamaguchi H, Giaime E, Boyle S, Kopan R, Kelleher RJ, 3rd and Shen J (2010) Loss of leucine-rich repeat kinase 2 causes impairment of protein degradation pathways, accumulation of alpha-synuclein, and apoptotic cell death in aged mice. *Proc Natl Acad Sci U S A* **107**:9879-9884.

Wang S, Liu Z, Ye T, Mabrouk OS, Maltbie T, Aasly J and West AB (2017) Elevated LRRK2 autophosphorylation in brain-derived and peripheral exosomes in LRRK2 mutation carriers. *Acta Neuropathol Commun* **5**:86.

West AB, Moore DJ, Biskup S, Bugayenko A, Smith WW, Ross CA, Dawson VL and Dawson TM (2005) Parkinson's disease-associated mutations in leucine-rich repeat kinase 2 augment kinase activity. *Proc Natl Acad Sci U S A* **102**:16842-16847.

Whiffin N, Armean IM, Kleinman A, Marshall JL, Minikel EV, Goodrich JK, Quaife NM, Cole JB, Wang Q, Karczewski KJ, Cummings BB, Francioli L, Laricchia K, Guan A, Alipanahi B, Morrison P, Baptista MAS, Merchant KM, Genome Aggregation Database Production T, Genome Aggregation Database C, Ware JS, Havulinna AS, Iliadou B, Lee JJ, Nadkarni GN, Whiteman C, andMe Research T, Daly M, Esko T, Hultman C, Loos RJF, Milani L, Palotie A, Pato C, Pato M, Saleheen D, Sullivan PF, Alfoldi J, Cannon P and MacArthur DG (2020) The effect of LRRK2 loss-of-function variants in humans. *Nat Med* **26**:869-877.

Zhao J, Molitor TP, Langston JW and Nichols RJ (2015) LRRK2 dephosphorylation increases its ubiquitination. *The Biochemical journal* **469**:107-120.

JPET Fast Forward. Published on January 28, 2021 as DOI: 10.1124/jpet.120.000217
This article has not been copyedited and formatted. The final version may differ from this version.

13. Footnotes

This work received no external funding.

No author has an actual or perceived conflict of interest with the contents of this article.

The authors would like to inform the reviewers that our colleague, Carrie Markgraf, has passed away.

Reprint requests should be directed to Dr. Matthew Fell, Merck Research Laboratories, Office 8-122, 33 Avenue Louis Pasteur, Boston, MA 02115; matthew.fell@merck.com.

JPET Fast Forward. Published on January 28, 2021 as DOI: 10.1124/jpet.120.000217
This article has not been copyedited and formatted. The final version may differ from this version.

14. Figure Legends

Fig. 1. LRRK2 kinase inhibitors MLi-2 and GNE-7915 induce histomorphological changes in mouse lung. (A) H&E stained sections revealed changes in lung morphology following 1 week of LRRK2 kinase inhibitor treatment. Arrows indicate slight enlargement of randomly scattered alveolar epithelial cells consistent with type II pneumocytes. (B) Immunohistochemical analysis of lung sections shows that enlarged vessels stain positive for proSP-C.

Fig. 2. Pharmacokinetic modelling to predict equivalent MLi-2 PO dosing regimen to recapitulate PD and lung results with 60 mg/kg/day in-diet (A) Unbound concentrations of MLi-2 following acute or chronic dosing. Mice were treated PO QD for 1 week (triangles) or in-diet with either 30 mg/kg/day (green circles) or 60 mg/kg/day (red circles) and plasma samples collected at multiple timepoints. Formation of enlarged lung inclusions only manifest when plasma levels were sustained at ≥10x the IC_{50} for MLi-2. (B) Prediction of MLi-2 plasma concentrations over time following PO dosing of MLi-2 BID. Red squares indicate actual plasma concentrations from test mice and the hatched line represents the minimal trough target exposure predicted to provoke the lung phenotype. (C) Analysis of target engagement, expressed as a ratio of pSer935 LRRK2/total LRRK2, or total LRRK2 (normalized to GAPDH) in lung. Mice dosed BID with 150 mg/kg MLi-2 showed robust inhibition of pSer935, equivalent to that seen following 60 mg/kg/day in-diet treatment. Total LRRK2 levels were not significantly changed in either tissue. (D) Quantification of proSP-C stained areas of lung using Halo image analysis. Both PO and in-diet treatment groups showed significant enlargement of type II pneumocytes. N=4-6 per group.

Fig. 3. Biochemical and histological characterization of lung from mice treated with GNE-7915 in-diet for 7 days. Western blot (A) and quantification (B) of lung samples in which GNE-7915 dose-dependently inhibited pSer935 LRRK2 levels (ratio of pSer935 LRRK2/total LRRK2, expressed as a percentage of the vehicle control group) while having no effect on total LRRK2 protein levels (normalized to GAPDH levels for each band). (C) pSer935 LRRK2 levels in lung versus unbound concentrations of GNE-7915 (10-300mg/kg/day) on day 7 of in-diet dosing. (D) GNE-7915 significantly increased area of type II pneumocytes as measured by IHC (proSP-C). Areas were quantified then normalized to the vehicle control group. N=4 per group.

Fig. 4. In-diet dosing with MLi-2 from 3 to 180 days induced modest changes to lung. Within 3 days of dosing, and continuing to day 180, 120mg/kg/day MLi-2 induced significant increases in proSP-C levels, as compared to the vehicle control group. Significant increases in the 60mg/kg/day group are seen after 7 days, peak at day 28, then revert to normal levels by day 180.

Fig. 5. Biochemical and histomorphological changes to lung following 1-6 months of MLi-2 dosing are reversible with 1-week washout. (A) Observed increases in type II pneumocyte size following 120mg/kg/day from 28 to 180 days were greatly reduced with 1 week compound washout. (B) Quantification of IHC staining for proSP-C showed significant increases in staining that reverted to baseline after cessation of MLi-2 dosing. (C) No change in surfactant secretion was detected in BAL fluid from mice dosed for 28 days, nor was any effect on compound washout noted. Hatched bars indicate washout of compound. Light bars = 60 mg/kg/day, dark bars = 120 mg/kg/day, hatched lines indicate washout arm. N=4-6 per group.

JPET Fast Forward. Published on January 28, 2021 as DOI: 10.1124/jpet.120.000217
This article has not been copyedited and formatted. The final version may differ from this version.

15. Table 1

Table 1. PK and lung data from mice treated for 7 days in-diet with a LRRK2 inhibitor

LRRK2 Compound	Dose (mg/kg/day)	Plasma (u, nM)	TE_{lung} % INH	-fold over TE_{lung} IC_{50}	Histopath (score per mouse)	Surfactant proSP-C % VEH
MLi-2	3	0.14	0	~	- - - -	~
	10	0.59	26	~	- - - -	~
	30	3.37	89	2.6	- - - -	103
	60	7.50	93	5.8	++++	113
	120	26.2	95	20.3	++++	121
GNE-7915	30	14.5	47	1.2	- - - -	102
	100	21.6	81	1.8	- - - -	104
	300	28.2	89	2.4	+ - - -	111

u= unbound concentration; TE= target engagement; INH= inhibition; VEH= vehicle; + positive lung finding; - negative lung finding

JPET Fast Forward. Published on January 28, 2021 as DOI: 10.1124/jpet.120.000217
This article has not been copyedited and formatted. The final version may differ from this version.

16. Figures

Figure 1

JPET Fast Forward. Published on January 28, 2021 as DOI: 10.1124/jpet.120.000217
This article has not been copyedited and formatted. The final version may differ from this version.

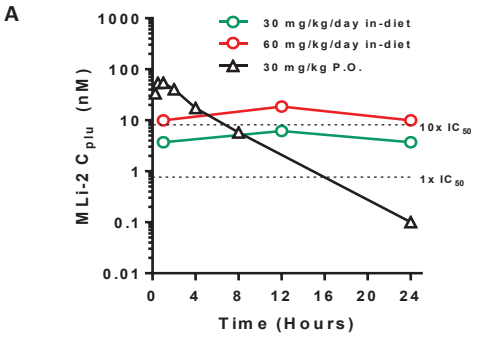

Figure 2

JPET Fast Forward. Published on January 28, 2021 as DOI: 10.1124/jpet.120.000217
This article has not been copyedited and formatted. The final version may differ from this version.

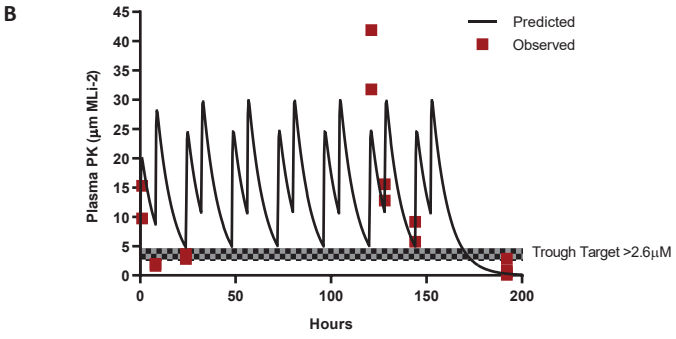

Figure 2

JPET Fast Forward. Published on January 28, 2021 as DOI: 10.1124/jpet.120.000217
This article has not been copyedited and formatted. The final version may differ from this version.

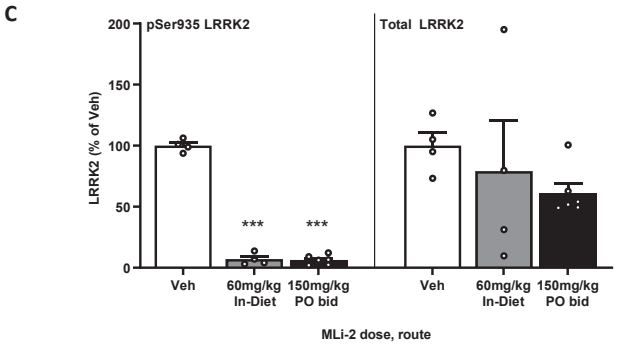

Figure 2

JPET Fast Forward. Published on January 28, 2021 as DOI: 10.1124/jpet.120.000217
This article has not been copyedited and formatted. The final version may differ from this version.

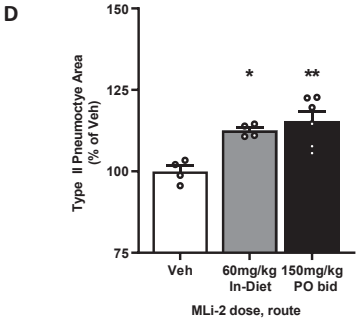

Figure 2

JPET Fast Forward. Published on January 28, 2021 as DOI: 10.1124/jpet.120.000217
This article has not been copyedited and formatted. The final version may differ from this version.

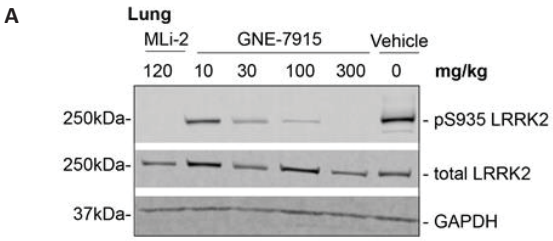

Figure 3

JPET Fast Forward. Published on January 28, 2021 as DOI: 10.1124/jpet.120.000217
This article has not been copyedited and formatted. The final version may differ from this version.

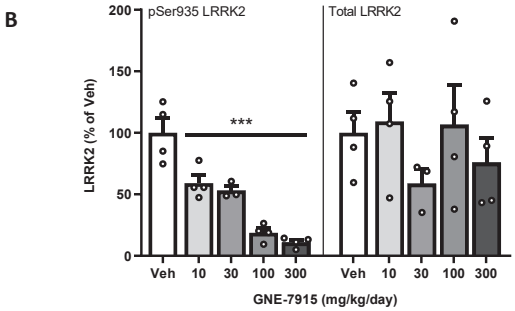

Figure 3

JPET Fast Forward. Published on January 28, 2021 as DOI: 10.1124/jpet.120.000217
This article has not been copyedited and formatted. The final version may differ from this version.

C

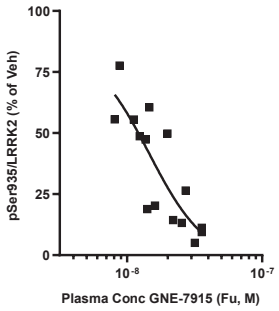

Figure 3

JPET Fast Forward. Published on January 28, 2021 as DOI: 10.1124/jpet.120.000217
This article has not been copyedited and formatted. The final version may differ from this version.

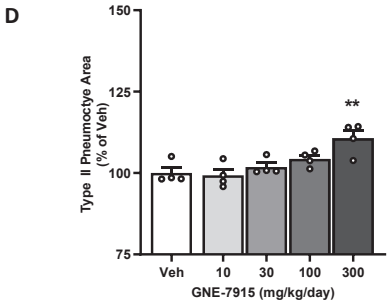

Figure 3

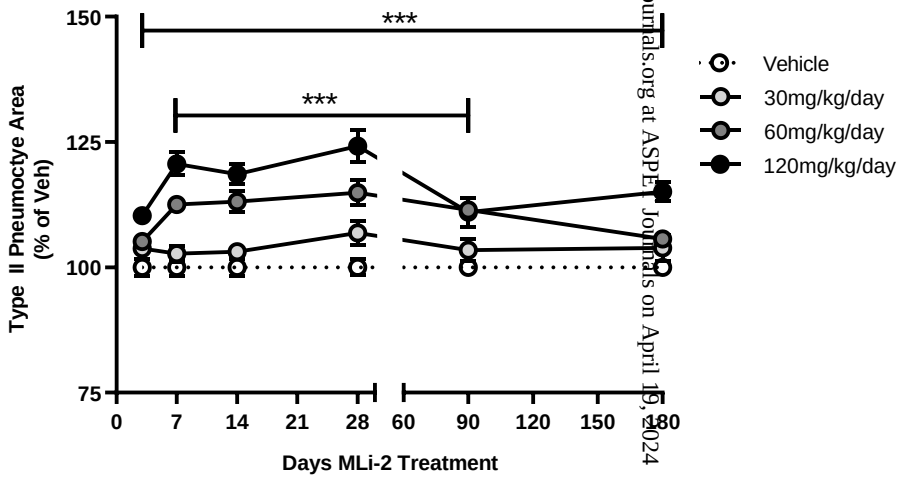

Figure 4

JPET Fast Forward. Published on January 28, 2021 as DOI: 10.1124/jpet.120.000217
This article has not been copyedited and formatted. The final version may differ from this version.

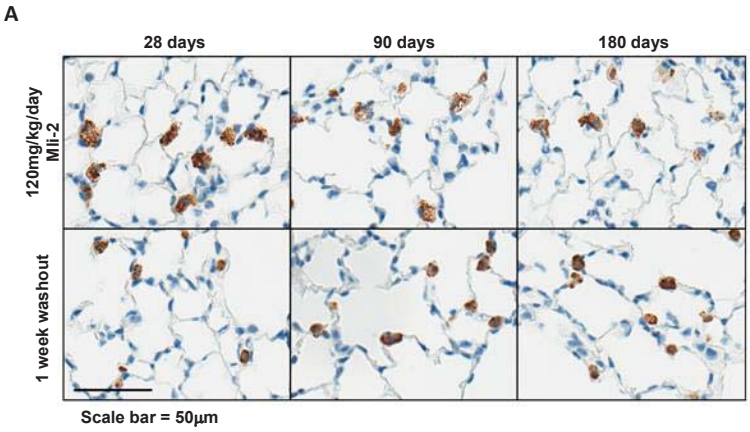

Figure 5

JPET Fast Forward. Published on January 28, 2021 as DOI: 10.1124/jpet.120.000217
This article has not been copyedited and formatted. The final version may differ from this version.

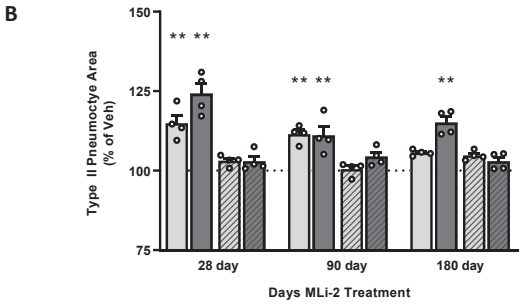

Figure 5

JPET Fast Forward. Published on January 28, 2021 as DOI: 10.1124/jpet.120.000217
This article has not been copyedited and formatted. The final version may differ from this version.

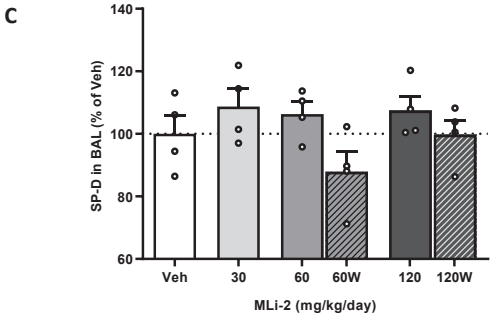

Figure 5